

# Beam Transfer

A. K. GARRISON  
GTRI, GEORGIA INSTITUTE OF TECHNOLOGY, ATLANTA, GA 30332

## F.1. INTRODUCTION

The beam transfer subsystem transfers the light beam from each telescope to the Optical Path Length Equalizer (OPLE) subsystem. The functionality of this subsystem and details of the subsystem design are presented here. Design options and risks are also discussed.

## F.2. FUNCTIONALITY

### F.2.1. General Considerations

The subsystem requirements are as follows:

1. The beam tube must transmit the light beam from each telescope to the OPLE.
2. The transmission process should provide minimum distortion of the wavefront (phase and amplitude) over the visible range of wavelengths (0.4 – 0.9 microns) and the IR (0.9 – 3.0 microns) so that there is negligible contribution to the system visibility error.
3. The first two requirements must be met given the environment and topography of the site.
4. The subsystem should have a mean time between failures of at least a year.
5. The subsystem must meet safety requirements, particularly those associated with vacuum systems and vacuum windows.

The layout of the subsystem is shown in Figure F.1. The position of each fixed telescope is shown with an open circle and the positions of the movable telescopes are shown with cross-hatch circles. The lines running from each of the circles to the center of the configuration represent the path of the beam transfer tubes. The values of “r” are the approximate distances of the telescopes from the configuration center. There are four beam tubes in the north leg and three each in the other two legs, for a total of ten beam tubes. The beam tubes to the sites for the movable telescopes will remain in place and be part of the permanent site to receive the movable telescopes. The length of each beam tube is given in Table F.1.

There were several trade studies carried out during the Phase A and Phase B design programs. The consideration of the type of vacuum joint to be used in joining the section of pipes was focused on a choice between the standard “O”-ring flange joint or the use of a neoprene sleeve that is clamped around the tube to provide a vacuum seal between the two ends of the pipe as they are butted together. The USNO/NRL group is a proponent of the neoprene gasket and have tested its leak rate in the laboratory. They find there is very little loss of vacuum from the one torr level in a week. The SUSI group chose the “O”-ring

**FIGURE F.1.** The beam tube subsystem layout.

flange method because it a reliable and standard method of making the joint. We have chosen the “O”-ring flange joints because we want a conservative design to give at least one year MTBF. Our beam tubes have more joints than in any other arrays presently under construction, so there is more chance for small leaks and we are concerned with the effects of UV radiation on the integrity of the neoprene. The ease of assembly of a large number of sections is also a factor that favors the “O”-ring flange. The results of another trade study on the window transmission versus costs will be given in the discussion of the beam tube windows. An extensive trade study of helium filled versus vacuum beam tubes was carried out in the Phase A design study and is described next.

The obvious choice for the beam tubes to take the beam from the telescope to the OPLE without distortion of the wavefront is an evacuated pipe with plane transmitting windows. However, there are several factors that make this obvious design problematic. The windows must be thick enough to provide a safe vacuum vessel, which means they will be thick enough to attenuate the beam and they might bow to give intolerable wavefront distortion. They must also be proof tested against implosion which adds to their cost. These problems could be eliminated if the vacuum were replaced with a gas inside the beam tube to make the pressure differential across the window small.

## BEAM TRANSFER SUBSYSTEM

**TABLE F.1.** Dimensions of the beam tubes

Telescope	Length (m)	Volume (m <sup>3</sup> )	No. of 20' sections
N1	200	5.0	33
N1'	41	1.0	7
N2	64	1.6	11
N3	14	0.3	2
E1	200	5.0	33
E1'	45	1.1	7
E2	111	2.8	18
W1	200	5.0	33
W1'	23	0.6	4
W2	87	2.2	14
TOTAL		24.6	162

### F.2.2. A Helium Alternative to Vacuum

Enclosing any gas in a thermally insulated container so that the gas is stagnant would probably provide low distortion of the wavefront as it passes through the tubes. However, the tubes will be exposed to sunlight during the day that will cause a temperature gradient from top to bottom of the tubes that could have a long decay time after sunset. Putting the tubes underground or using a temperature control system for the tubes was considered too expensive and greatly complicated troubleshooting and leak checking.

Thus it was decided to quantify, in a laboratory experiment, the distortion of the wavefront as it was transmitted through a horizontal, gas-filled tube that was subject to a temperature difference across the diameter. The following presents the procedure for the evaluation, the results and conclusions.

The purpose of the experiments was to compare the size of the perturbations of the light beam wavefront caused by a temperature gradient across a tube containing air or helium. As seen in Figure F.2, the variation of the refractivity for helium with temperature is an order of magnitude less than the variation for air. This fact, combined with the relatively modest expense of helium, makes it attractive as a possible substitute for a vacuum system while also solving the thick window problem. The results of the experiments would give important data for making design decisions on the light beam tubes.

A steel pipe made for industrial use that was 10 ft long and 10 in in diameter with 0.5 in walls was sealed at the ends with plate glass and silicon sealant. Since the windows would not support atmospheric pressure, the tube could not be evacuated before introducing the helium. Thus a simple way of increasing the fraction of helium in the tube and a simple way of measuring its concentration was needed. Initially the helium was introduced from a high pressure cylinder by connecting a hose to the pressure reduction valve, inserting it into the pipe through a hole in the side, controlling the flow with the valve and attempting to displace the air. Attempts to deduce the fraction of helium in the pipes by measuring the resonant frequency of the pipe closed at one end, and hence obtain the speed of sound for the gas mixture, were not successful because extra resonances were found as the helium was introduced. As expected, it was difficult to displace air effectively in pipes of this

THE CHARA ARRAY

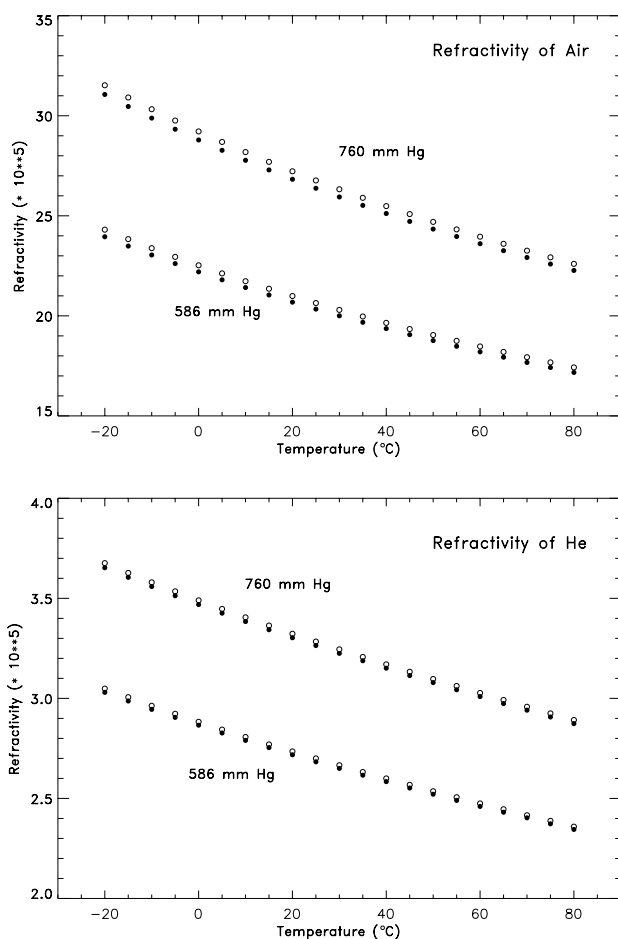


**FIGURE F.2.** The refractivity of helium and air are compared at visible ( $6000\text{\AA}$  – open circles) and infrared ( $2.2\ \mu\text{m}$  – filled circles) wavelengths under two pressure conditions as a function of temperature. Helium is, under all circumstances, about an order of magnitude more favorable than air in terms of refraction index.

diameter, so only small amounts of helium were introduced. It was concluded that the spurious resonances may have been due to stratification of the air and helium in the tube. Another method of introducing the helium was to open one end of the pipe and pull a ball of the right size to serve as a piston through the pipe and let the helium fill in back of it, but again the spurious resonances were observed. The most suitable method that was found was to fill balloons with the helium, fill the tube with them by inserting them into the tube from an open end, seal the window and pull a device on a string through the pipe to burst the balloons. In this way the amount of air displaced by the balloons could be estimated fairly accurately to be about 80%.

A maximum temperature difference across the pipe of about  $44^\circ\text{C}$  was obtained by fastening two 800 watt heating tapes along the top. The temperature was measured with copper constantan thermocouples placed at several locations along the top and bottom of the pipe.

The perturbation of the wavefronts was measured using a small HeNe laser with the beam

## BEAM TRANSFER SUBSYSTEM

expanded to 2.5 cm diameter at one end of the pipe and a lateral shearing interferometer at the other end. The intensity of the fringes formed by the interferometer was measured using a phototransistor in the fringe pattern and plotting its output on an  $x - y$  recorder. In this arrangement perturbations of the wavefront cause the fringe spacing to change, which varies the fringe intensity monitored by the phototransistor. The minimum fringe intensity change that could be observed was about 0.04 of the intensity difference between dark and bright fringes. Using the records of the output, one can compare the effects using helium and air in the pipe.

There were two categories of results: a slow drift in one direction of the phototransistor output as the temperature gradient increased, and a more rapid random variation in output as the temperature gradient increased. The size of the maximum drift for the helium was about one third that for air. The random fluctuations in air are not observable below a temperature difference across the tube of 16° C. The maximum fluctuation was about 0.33 of the fringe intensity difference and the average was about 0.1. The average fluctuation did not change with temperature gradients from 22° to 40° C across the pipe. With the helium in the pipe the random fluctuations were not observable below a temperature difference of 19° C across the pipe. The maximum fluctuations were about 0.4 of the fringe intensity difference. The average increased from 0.04 to about 0.1 as the temperature gradient increased from 19° to 33° C across the pipe.

The slow drift in the fringe spacing is thought to arise from the change in the wavefront curvature as the average refractivity of the air or the helium-air mixture changes with temperature. The change is smaller for helium as expected but is not as small as the ratio of the change in refractivity with temperature from helium to air because of the incomplete displacement of air by helium. The rapid random changes are attributed to turbulence caused by the temperature gradient. The helium-air mixture gave as much, if not more, wavefront distortion of this type as did the air. Because the width of the phototransistor sensitive area was about the same as that of a fringe, one cannot accurately deduce the amount of wavefront distortion from the intensity changes measured by the phototransistor, although a visual estimate of the maximum shift of fringe spacing was about 0.25 of the fringe spacing. This corresponds to an intensity change of 0.5 the difference between the bright and dark fringe. A change in the fringe spacing by 25% corresponds to a change in the radius of curvature of the wavefront planes was also observed but not measured. If all the air were replaced by helium, this distortion may be reduced by 20%, but increasing the length of the beam tube to 200 m would surely increase the size of the distortion to more than overcome this decrease. It was therefore concluded that helium-filled pipes would not preserve the shape of the incoming wavefronts unless the temperature difference across the pipe is less than 19° C or 34° F. It is likely that titanium oxide paint will provide the needed thermal uniformity of the pipe. Any effective way of introducing helium into the pipes seems to necessitate a vacuum system to purge the air from the system initially. Therefore helium as an alternative optical medium does not provide any economic advantages over a straightforward vacuum system. Furthermore, as is described in Section F.3.2, thin windows are more difficult to manufacture and hence more costly than thicker windows.

### F.2.3. General Conclusions

The conclusions of these trade studies indicate that the beam transfer subsystem should have evacuated light pipes with vacuum tested windows and "O"-ring flange joints in order to meet the subsystem requirements with minimum risk. With these conclusions in mind, the design of the subsystem is organized around three assemblies: light pipes, light pipe support

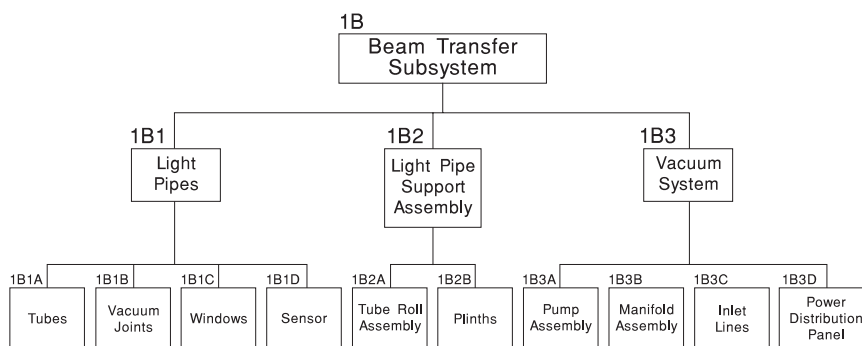


**FIGURE F.3.** The beam transfer subsystem hardware tree.

assembly, and vacuum system. Figure F.3 shows the hardware tree for the subsystem to the subassembly level. The following section discusses each of these assemblies in detail.

### F.3. ASSEMBLY DESCRIPTIONS

#### F.3.1. Light Pipe Assembly

The light pipe assembly, 1B1, consists of the beam tubes, the vacuum joints, beam tube windows, and vacuum gauge.

The beam tubes are to be steel pipes 20 ft long and 7 in (17.8 cm) ID with approximately 0.25 in walls. The length is chosen for convenience of transporting and handling. The inside diameter is designed to accommodate the 12.5 cm diameter collimated beam coming from the telescope and beam wander of  $\pm 26''$  after the telescope which corresponds to  $\pm 2.6$  cm at the end of the 200 m tube. This tolerance for beam wander without hitting the side of the tube is designed to aid the alignment procedures.

As mentioned above, each 20 ft section will have an “O” flange on one end and a plane flange on the other. However, each 20 ft section of the steel pipe will expand 0.09 ft for a 60° F temperature increase so every ten sections will have a 1 in long vacuum bellows expansion joint rather than the “O”-ring flange. One expansion joint will be put in pipes of less than ten sections.

#### F.3.2. Vacuum Windows

The minimum diameter of the light pipe window is determined by the clear aperture required to accommodate the maximum beam deflection of  $\pm 8''$  for the atmospheric tip-tilt correction mirror at the telescope end of the tubes. This gives a beam displacement of  $\pm 0.8$  cm at the end of the 200 m tube. The telescope tracking error is estimated to be  $\pm 1''$  with active control so the tip-tilt determines the minimum clear aperture of the window, assuming the beam is aligned along the axis of the tube, to be 14.1 cm or about 5.5 in. The window will be mounted on an “O”-ring flange that has a central hole slightly larger than 5.5 in and clamped with a ring clamp.

The thickness of the window is a trade between the vacuum requirements and the inverse dependence of transmission on thickness. The minimum thickness for vacuum safety depends on the kind of material used for the window and the surface flaws introduced by the

## BEAM TRANSFER SUBSYSTEM

polishing techniques used. Because surface flaw size is critical in determining the strength of glass, the windows should be proof-tested before they are installed in the facility. This proof testing will add to the cost of the facility, but is more than justified in reducing the risk of injury or death.

Glass strength has a time dependence for both static and dynamic loading. For a constant load, failure occurs after a period of time at load that depends on the applied load. Failure is due primarily to fracture; the applied load causes propagation of small surface cracks until catastrophic failure occurs. In addition to surface flaw size, static fatigue of glass is dependent on the environment. Static fatigue does not occur in vacuum, and water or acids/alkalines must be present for fatigue to occur. The window surface exposed to the atmosphere will suffer these environmental effects, but fortunately this surface is in compression when the window is loaded. Glass is very much stronger in compression than in tension.

It may seem that quantifying the strength of the windows is a hopeless task, but much knowledge has been developed over the last few decades that allows the strength to be quantified statistically. The crack propagation velocity has been determined for certain environmental conditions. If the stress state and initial flaw size are known, a time to failure prediction can be made. Since the initial critical flaw size cannot be determined by visual inspection, a proof test is used to qualify the window.

The window is mounted in a test chamber and the pressure differential is brought to several times the differential the window will see in service. The window is held at this differential for a period of time, and then the differential is brought to zero. If the window did not fail during the proof test a reliable size estimate of the largest flaw on the window surface can be made. With this information an estimate of the time to failure can be made. The proof test does not reduce the lifetime of the window below that for an untested window. There is always the chance the window may be destroyed in the test due to the overpressurizing, but this is the price paid for safety and reliability. There is currently no non-destructive test to determine the presence or size of critical surface flaws.

Since the vacuum proofing will not be done until a final decision is made on the material or materials for the window, an exact thickness of the window is not determined at this time. However, a working thickness of 25 mm has been chosen for consideration of the transmission properties of various window materials. This thickness gives a deflection of  $0.3 \mu\text{m}$  at the center of the window due to atmospheric pressure and assuming a nominal value for Young's modulus for glass and a supporting radius of 73 mm.

Two materials are being considered at this time as possible candidates for windows. SK-2 glass from Schott and fused silica, infrasil from Heraeus. We have calculated the total transmission of a 25.4 mm thick sample of each of these materials with a  $\text{MgF}_2$  coating on both surfaces for wavelengths from 0.4 to 2.5 microns. The results of these calculations are shown in Figure F.4. From these considerations it is obvious that the infrasil is the choice for the window. Exotic coatings of two or more dielectrics were considered, but the coating houses we talked to discouraged this because of price and reliability in reproducing the coatings. The final choice between these two will be made using cost, polarization effects and vacuum proofing as discriminants.

Each tube will have a pirani vacuum gauge that will monitor the pressure in the tube. The pirani gauge controller will interface with the System Control Computer Subsystem so that the pressure in each tube is recorded in the central control room.

Figure F.5 shows the parts of the subassemblies for the light pipe assembly that have been

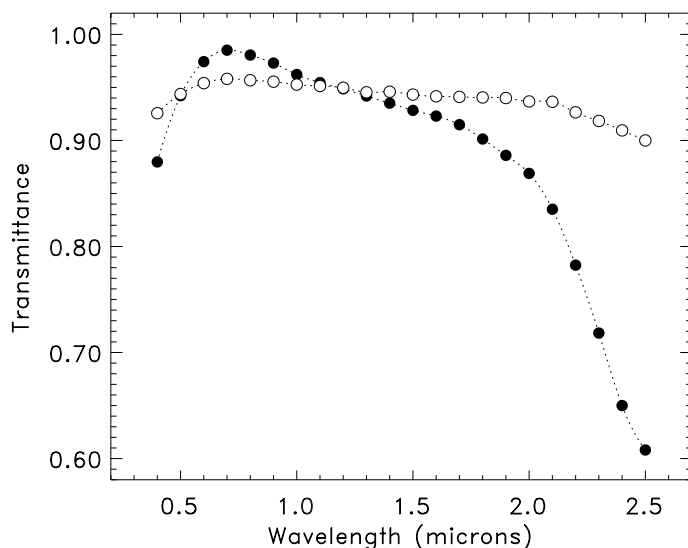


**FIGURE F.4.** Total transmission versus wavelength for Schott SK-2 glass (filled circles) and Heraeus Infrasil fused silica (open circles).

discussed in the paragraphs above.

### F.3.3. Support Assembly

The light pipe support assembly consists of support plinths and a tube roll assembly that holds the tubes on the support and allows for expansion. The hardware tree for these subassemblies is shown in Figure F.5. The plinths will be reinforced concrete piers with a steel cross piece and the plinths will be spaced approximately every 20 ft along each of the three arms of the interferometer. A drawing of a pier is shown in Figure F.6. The steel cross piece of WF 6×15 steel will support three or four tubes with the pipe roll assemblies.

The footing slab for the piers must be poured first with reinforcing stubbed in for the vertical piers and then vertical forms built and the piers poured. The complete structure might not be poured at once because the hydrostatic pressure may be too great for standard forms. The height of the piers will be adjusted for the terrain and a final leveling adjustment can be made with the pipe roll assembly.

At one support near the center of each light pipe run, the pipe will be clamped to the support rather than being placed on rollers. This should distribute the expansion uniformly over the rollers.

### F.3.4. Vacuum System

The vacuum system assembly consists of the pump assembly, the manifold assembly, the inlet lines and the power distribution panel. Figure F.7 shows the parts of these subassemblies. The pumps, manifold and distribution panel will be housed in a single small building away from the telescopes. The inlet lines will run to each of the ten light pipes for evacuation. The pumps will be used to evacuate the tubes to approximately 1 torr pressure, and

## BEAM TRANSFER SUBSYSTEM

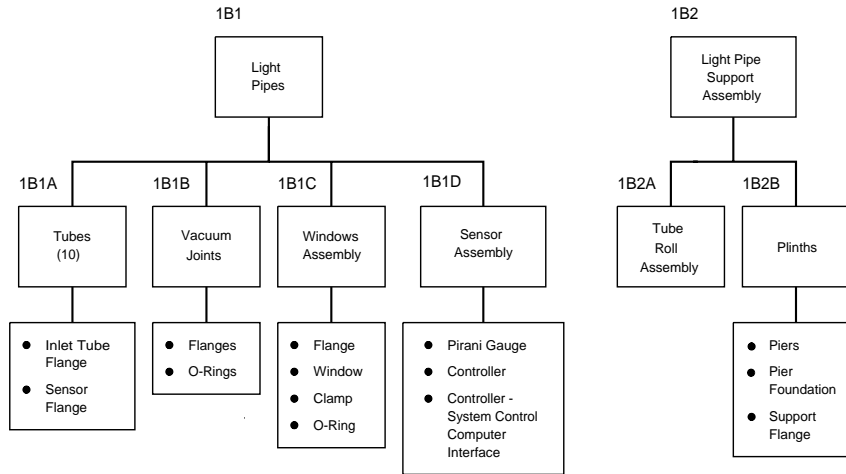


**FIGURE F.5.** Hardware tree for light pipes and support assemblies.

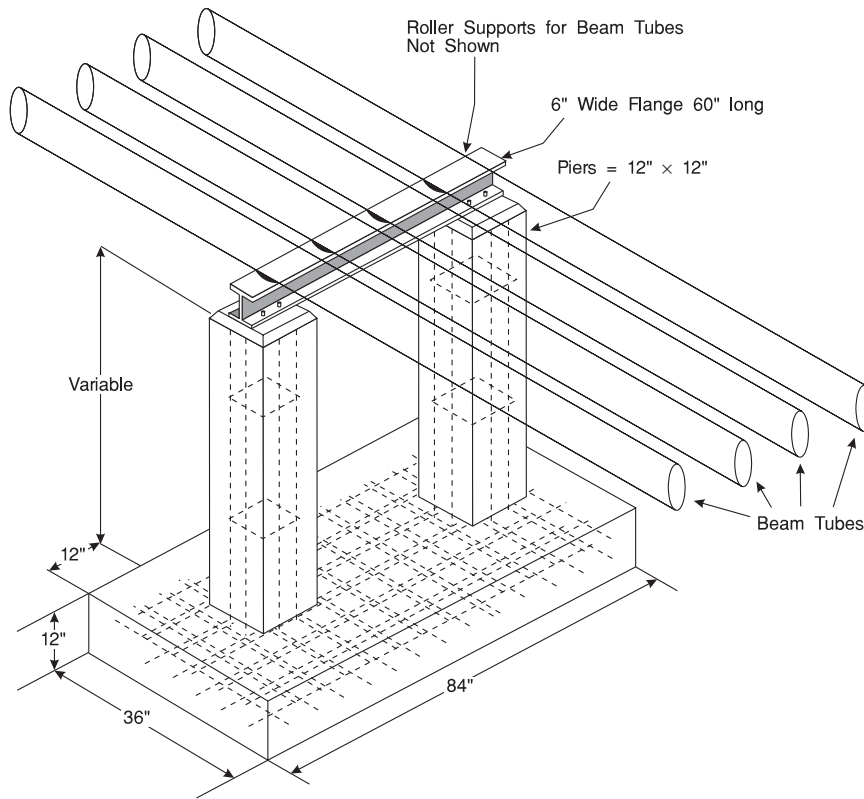
then gate valves on each inlet tube will be closed to isolate each light pipe. The pumps will not run during observation so that vibration and thermal turbulence from the pumps will not be a problem. A helium leak detector will be used during assembly and during maintenance of the subsystem to reduce the leak rate to a value that provides 1 torr pressure without pumping for several days at least.

Figure F.8 shows a schematic of the vacuum system designed in consultation with engineers from Leybold-Heraeus Corporation. It is recommended that an adsorption trap be placed in the foreline rather than the RST refillable trap to assure that all the backsteaming forepump oil is removed from the vacuum side. Oil cannot be tolerated on the inside of the pipe windows.

The trap will be the only vacuum system component that has a conductance that will decrease the D90A pumping speed. Using the vendor's values of pumping speed of the D90A as 191/s at 1 torr and the trap conductance as 121/s, one gets an effective pumping speed of 71/s. The time required for one pump to reduce the pressure in the entire light pipe volume of  $2.5 \times 10^4$  l from atmospheric to 1 torr pressure is about 6.5 hours assuming a clean system with no outgasing. The two pumps in the suggested system would take about 3 hours.

The pirani gauges on the manifold and the electropneumatic gate valves on the inlet lines will be interfaced to the System Control Computer Subsystem so that the pressure in the manifold can be monitored in the control room and the gate valves opened and closed from there also. The electrical power to the pumps will also be controlled from the control room through a power distribution panel-system control computer interface.

# THE CHARA ARRAY



**FIGURE F.6.** Support plinth for light pipes.

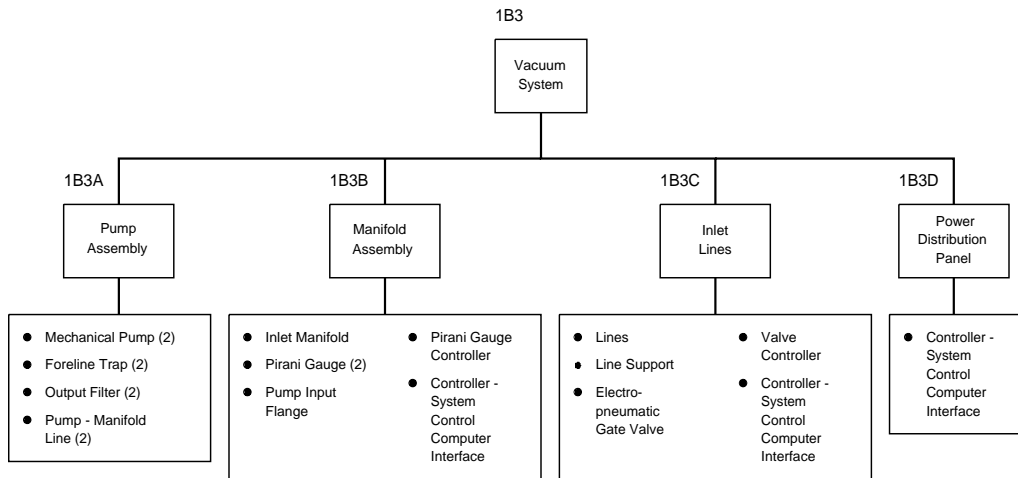


**FIGURE F.7.** Hardware tree for vacuum system.

# BEAM TRANSFER SUBSYSTEM

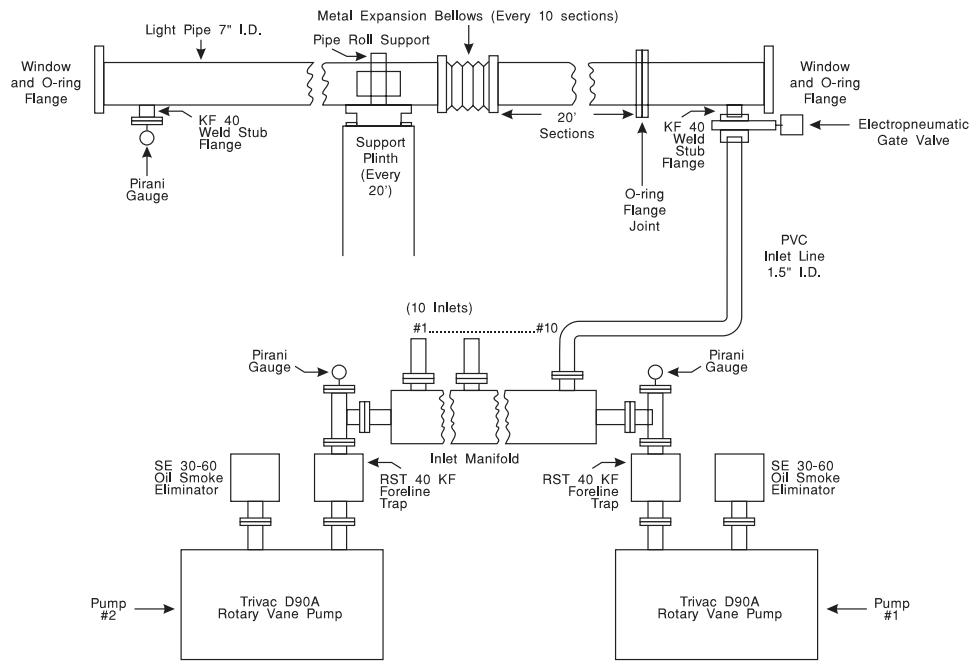


**FIGURE F.8.** Schematic of the vacuum system.